Available online at www.sciencedirect.com
ScienceDirect
Journal of Sound and Vibration 306 (2007) 136–152
JOURNAL OF SOUND AND VIBRATION
www.elsevier.com/locate/jsvi

Suppressing self-excited vibrations by synchronous and time-periodic stiffness and damping variation

Fadi Dohnal

Institute of Sound and Vibration Research, University of Southampton, Highfield, SO17 1BJ, UK

Received 22 December 2006; received in revised form 2 May 2007; accepted 15 May 2007
Available online 2 July 2007

Abstract

Stability investigations on vibration suppression employing the concept of actuators with variable stiffness and damping elements are presented. Systems with two and more degrees of freedom with linear spring- and damping-elements are considered, that are subject to self-excitation as well as parametric excitation by simultaneous stiffness and damping variation. General conditions for full vibration suppression are derived analytically by applying a singular perturbation method of first order. These conditions naturally lead to the terms of parametric resonance and anti-resonance and enable a stability classification with respect to the parametric excitation matrices. The results are compared to former investigations of systems with a pure stiffness variation and a pure damping variation in time. While a specific parametric stiffness or damping excitation may suppress the system vibrations successfully, the interaction of both excitations modifies the formerly gained stability regions in the system parameter space. The analytical predictions are verified for exemplary systems by exact numerical time integration. These basic results obtained can be used for design of a control strategy for actuators with synchronously variable stiffness and damping elements to suppress transient vibrations.

1. Introduction

The main objective of this contribution is to investigate the phenomenon of full suppression of self-excited vibrations by means of a special kind of parametric excitation. Self-excited vibrations represent a dangerous phenomenon in many engineering fields. Self-excitation of a structure can be caused for example by a steady wind flow or by dry friction. The self-excitation mechanism considered here is of linearised van der Pol or Rayleigh type. Both types lead to a linear but negative damping coefficient in the main diagonal of the damping matrix. A quite interesting active vibration suppression mechanism is the usage of parametric excitation. A parametric excitation may appear by harmonic variations of one or more system parameters. The resulting equations of motion are coupled linear differential equations with time-periodic coefficients of the form

$$\mathbf{M}(\eta\tau)\ddot{\mathbf{x}}(\tau) + \varepsilon\mathbf{C}(\eta\tau)\dot{\mathbf{x}}(\tau) + \mathbf{K}(\eta\tau)\mathbf{x}(\tau) = \mathbf{0}, \tag{1}$$

with the time τ, the parametric excitation frequency η, the position vector $\mathbf{x}$ and a scaling factor ε. The matrices $\mathbf{M}$, $\mathbf{C}$ and $\mathbf{K}$ correspond to the mass/inertia, damping and stiffness coefficients.

E-mail address: fd@isvr.soton.ac.uk

0022-460X/$ - see front matter © 2007 Elsevier Ltd. All rights reserved.
doi:10.1016/j.jsv.2007.05.029

There are several publications dealing with single or coupled differential equations having a time-periodic coefficient, i.e. Refs. [1–6], and the literature cited therein. The main focus of these works is the destabilising effect of a parametric excitation. Boundary curves of unstable parameter regions caused by parametric excitation are determined—the so-called parametric resonances. For systems with one degree of freedom these analyses lead to the famous Mathieu, Hill or Meissner equation. In these studies, for an additional, positive damping coefficient stabilising by parametric excitation is possible for systems that are similar to the classical inverse pendulum problem. A stability analysis of systems with one degree of freedom that are under the influence of parametric excitation as well as self-excitation can be found in Ref. [7].

The mechanism of damping by parametric excitation as proposed here is based on the effect of coupling modes by parametric excitation, which is quite different to the stabilisation of the inverse pendulum. Contrary to the inverse pendulum, the minimum model possesses two degrees of freedom. The phenomenon that full suppression of self-excited vibrations can be achieved by interaction with parametric excitation was discovered by A. Tondl in monograph [8]. The conditions for full vibration suppression have been formulated mathematically in Ref. [9] and later, using another approach, in Refs. [10–12]. It was found that self-excited vibrations can be fully cancelled by parametric excitation within a frequency interval near a parametric combination resonance frequency of the summation- or difference-type, as defined in Ref. [3]

$$\eta \approx |\Omega_1 \mp \Omega_2|/N, \quad N = 1, 2, \ldots, \tag{2}$$

wherein frequencies Ω_1 and Ω_2 are two undamped natural frequencies of the system and η is the frequency of the parametric excitation. A specific parametric excitation that stabilises an otherwise unstable system is called to be at parametric *anti*-resonance. The main contributions with respect to parametric anti-resonances and a negative damping coefficient can be found in Refs. [8–11,13–15]. Numerical verification of damping by parametric stiffness excitation can be found in Refs. [14,16] or Ref. [15]. Finally, first experimental results of damping by parametric stiffness excitation of artificial lumped mass systems with two degrees of freedom can be found in Refs. [17,18] showing great potential of being applied in practical applications. The main benefit of the periodic open-loop control of one or more physical parameters is that no feedback of the system response is needed, which differs from established work on periodic feedback control, see e.g. Ref. [19].

This method of suppressing self-excited vibrations has been studied for the case of a harmonic *stiffness* variation in Refs. [9,14,15]. The first works within this scope dealing with a time-periodic *damping* coefficient in combination with a negative damping coefficient can be found in Refs. [15,20]. The investigation of parametric anti-resonances in case of a variation of all physical properties—a simultaneous single-frequency variation of stiffness, damping and inertia coefficients—can be found in Ref. [15]. The actual contribution examines the combination of two types of parametric excitation, a simultaneous and synchronous stiffness and damping variation as initially investigated in Ref. [21]. To understand the potentials and limitations in the application field of damping by parametric excitation, the following study examines the stability boundary curves in the system parameter space.

The interaction between parametric stiffness and damping variation is of great importance for implementations of parametric excitation, since, except for some generic cases, it is rather difficult to control a single physical property without changing other properties in a specific system. In practical applications this type of variation may appear quite naturally, since the realisation of a mechanical device for stiffness variation almost certainly induces also a change of its damping with the same phase, synchronously, as its stiffness. An easy to imagine physical example is a beam with a time-varying length. Varying the length periodically causes a periodical change of the bending stiffness of the beam. Simultaneously, the structural damping is varied periodically, because the part of the beam that experiences vibrations changes periodically, too. Both variations proceed synchronously.

In the following an analytical stability analysis is performed for a system in normal form and possessing two degrees of freedom. Thereafter, stability conditions are given for systems with multiple degrees of freedom and general conclusions are drawn. Finally, two numerical examples are discussed and compared to the analytical predictions.

2. Stability analysis

Linear differential equations with time-dependent, but periodic coefficients cannot be solved analytically exact. Sometimes an exact solution cannot be obtained for a differential equation and an approximate solution must be found. Other times, an approximate solution may convey more information than an exact solution. In this study, the exact solution is approximated by performing a perturbation technique as used in the literature in various fields of physics. Famous representatives of these techniques are: harmonic balance (or two-timing), Poincaré–Lindstedt method, averaging method, method of multiple scales or successive approximation to mention the most popular ones. A general survey of these methods can be found in Refs. [22–24]. The method of vibrational mechanics as proposed in Ref. [25] leads to demonstrative physical interpretations if the fast and the slow motions are coupled additively, but this method is not capable of providing a solution if the slow and the fast motion are coupled multiplicatively, as it is the case in Eq. (1). The methods above assume that the scaling factor ε is small. A method for arbitrary size of ε based on the original Lyapunov transformation can is developed in Ref. [26] but leads to expressions that are hard to interpret. High-frequency effects as outlined in Ref. [27] are not considered here, since damping by parametric excitation is mainly effective in the low-frequency domain in the range of the first modes of a system. The method chosen here is the averaging method, see Ref. [28], which is a method with a strong mathematical background. The approximations to the solution will be derived for a first-order perturbation and are only valid in a region and on the time scale $1/\varepsilon$. Only systems with distinct eigenvalues are considered.

2.1. Equations of motion

For the case of a synchronous damping and stiffness variation the inertia matrix is kept constant while the stiffness and damping matrices are varied periodically with a frequency η

$$\mathbf{M}(\eta\tau) = \mathbf{M}_0, \quad \mathbf{K}(\eta\tau) = \mathbf{K}_0 + \varepsilon\mathbf{K}_t\cos(\eta\tau), \quad \mathbf{C}(\eta\tau) = \mathbf{C}_0 + \varepsilon\mathbf{C}_t\cos(\eta\tau), \tag{3}$$

where the index 0 denotes the constant part and the index t the time-dependent part of the corresponding matrix. Rescaling the time-dependent damping matrix for small values $\varepsilon\mathbf{C}_t \mapsto \mathbf{C}_t$ in order to capture the influence of $\mathbf{C}_t$ within a first-order analysis, the general linear equations of motion in Eq. (1) simplify to

$$\mathbf{M}_0\mathbf{z}''(\tau) + \varepsilon\mathbf{C}_0\mathbf{z}'(\tau) + \mathbf{K}_0\mathbf{z}(\tau) = -\varepsilon\{\mathbf{C}_t\dot{\mathbf{z}}(\tau) + \mathbf{K}_t\mathbf{z}(\tau)\}\cos(\eta\tau). \tag{4}$$

Restricting the following study to systems with distinct eigenvalues, the equations of motion can be transformed to the normal form:

$$\mathbf{z}''(\tau) + \varepsilon\Theta\mathbf{z}'(\tau) + \Omega^2\mathbf{z}(\tau) = -\varepsilon\{\mathbf{R}\mathbf{z}'(\tau) + \mathbf{Q}\mathbf{z}(\tau)\}\cos(\eta\tau), \tag{5}$$

where

$$\Omega^2 = \mathbf{T}^{-1}\mathbf{M}_0^{-1}\mathbf{K}_0\mathbf{T}, \tag{6}$$

$$\Theta = \mathbf{T}^{-1}\mathbf{M}_0^{-1}\mathbf{C}_t\mathbf{T}, \quad \mathbf{Q} = \mathbf{T}^{-1}\mathbf{M}_0^{-1}\mathbf{K}_t\mathbf{T}, \quad \mathbf{R} = \mathbf{T}^{-1}\mathbf{M}_0^{-1}\mathbf{C}_t\mathbf{T}. \tag{7}$$

The transformation matrix $\mathbf{T}$ is defined by the diagonal matrix of squared natural frequencies Ω^2. Using Einstein summation, a convention that repeated indices are implicitly summed over, Eq. (5) can be rewritten in the comprehensive form

$$z_i''(\tau) + \Omega_i^2 z_i(\tau) = -\varepsilon\{\Theta_{ij}z_j'(\tau) + \{R_{ij}z_j'(\tau) + Q_{ij}z_j(\tau)\}\cos(\eta\tau)\}. \tag{8}$$

Herein i is the free index. For a system with two degrees of freedom $i,j = 1,2$.

From now on the factor ε is assumed to be small. The approach presented bellow is a natural extension of the procedure applied in Ref. [11] or Ref. [10].

2.2. Transformation and averaging

Applying a time transformation to Eq. (8) in order to normalise the frequency η to become one on the chosen time scale gives

$$\eta\tau \mapsto t, \quad ()' = \frac{\mathrm{d}}{\mathrm{d}\tau}, \quad ()^{\cdot} = \frac{\mathrm{d}}{\mathrm{d}t}, \quad z_i(\tau) \mapsto z_i(t). \tag{9}$$

Allowing a small detuning of first order near η_0 of the form

$$\eta = \eta_0 + \varepsilon\sigma + \mathcal{O}(\varepsilon^2), \tag{10}$$

dividing Eq. (8) by η^2 and expanding the coefficients to Taylor series for small values of parameter ε gives

$$\ddot{z}_i + \varpi_i^2 z_i = -\frac{\varepsilon}{\eta_0^2}\{\eta_0 \Theta_{ij}\dot{z}_j + \{\eta_0 R_{ij}\dot{z}_j + Q_{ij} z_j\}\cos t - 2\Omega_i \varpi_i \sigma z_i\} + \mathcal{O}(\varepsilon^2) \tag{11}$$

with the abbreviations $\varpi_i = \Omega_i/\eta_0$. For a *first-order approximation* all terms of higher order than ε are neglected. Similar to the classical method of estimating the particular solution from the homogenous solution by variation of parameters, the coordinate transformation

$$z_i = u_i \cos \varpi_i t + v_i \sin \varpi_i t, \quad \dot{z}_i = -u_i \varpi_i \sin \varpi_i t + v_i \varpi_i \cos \varpi_i t \tag{12}$$

is performed that fulfills the unperturbed equations ($\varepsilon = 0$). By introducing the abbreviations $s_i = \sin \varpi_i t$ and $c_i = \cos \varpi_i t$ Eq. (11) is transformed to

$$\dot{u}_i = -\frac{\varepsilon}{\eta_0^2 \varpi_i} f_i(\mathbf{u}, t) s_i, \quad \dot{v}_i = \frac{\varepsilon}{\eta_0^2 \varpi_i} f_i(\mathbf{u}, t) c_i \tag{13}$$

with the state vector $\mathbf{u} = [u_1, v_1, u_2, v_2]^{\mathrm{T}}$ and

$$f_i(\mathbf{u}, t) = -\eta_0(\Theta_{ij} + R_{ij}\cos t)(-u_j \varpi_j s_j + v_j \varpi_j c_j) - Q_{ij}\cos t\ (u_j c_j + v_j s_j) + 2\Omega_i \varpi_i \sigma(u_i c_i + v_i s_i).$$

The functions $f_i s_i$ and $f_i c_i$ on the right-hand side of this system of equations are quasi-periodic and can be split into a finite sum of N periodic terms with periods T_k in t. For this case *averaging method in the general case* from Ref. [28] can be applied

$$\dot{\hat{u}}_i = \varepsilon \sum_{k=1}^{N} \frac{1}{T_k} \int_0^{T_k} \tilde{F}_{i,k}^{s}(\hat{\mathbf{u}}, t)\,\mathrm{d}t, \quad \dot{\hat{v}}_i = \varepsilon \sum_{k=1}^{N} \frac{1}{T_k} \int_0^{T_k} \tilde{F}_{i,k}^{c}(\hat{\mathbf{u}}, t)\,\mathrm{d}t, \tag{14}$$

where the difference between the solutions $\mathbf{u}$ of the original and $\hat{\mathbf{u}}$ of the averaged system is of order ε, $\hat{u}_i(t) - u_i(t) = \mathcal{O}(\varepsilon)$, on the time scale $1/\varepsilon$. The integration over T_k is carried out for fixed average values $\hat{\mathbf{u}}$.

Hence, for averaging first the periods of the right-hand sides of Eq. (13) have to be determined. With the help of decomposition theorems the arising products of the trigonometric terms on the right-hand sides of Eq. (13) can be rearranged as a sum of basic trigonometric terms. For this simple system with two modes 12 different periods arise. Averaging over a basic trigonometric term yields always zero, except for the case where a term becomes resonant, i.e. the argument of a cosine function vanishes.

The following study will be performed for the case of a parametric combination frequency of first-order as defined in Eq. (2) for $N = 1$. Combination resonances of higher-order N may be applied to suppress self-excited vibrations, too, but in general their effectiveness is negligible compared to $N = 1$. Averaging Eq. (13) for $N = 1$ results in

$$\begin{aligned}
\dot{\hat{u}}_i &= \frac{\varepsilon}{\eta_0^2 \varpi_i}\left\{-\frac{\eta_0}{2}\Theta_{ii}\varpi_i \hat{u}_i \pm \frac{Q_{ij}}{4}\hat{v}_j \mp \eta_0 \frac{R_{ij}}{4}\hat{u}_j - \Omega_i \varpi_i \sigma \hat{v}_i\right\},\\
\dot{\hat{v}}_i &= \frac{\varepsilon}{\eta_0^2 \varpi_i}\left\{-\frac{\eta_0}{2}\Theta_{ii}\varpi_i \hat{v}_i - \frac{Q_{ij}}{4}\hat{u}_j - \eta_0 \frac{R_{ij}}{4}\hat{v}_j + \Omega_i \varpi_i \sigma \hat{u}_i\right\},
\end{aligned} \tag{15}$$

where the upper signs correspond to $\eta_0 = |\Omega_1 - \Omega_2|$ and the lower signs to $\eta_0 = \Omega_1 + \Omega_2$. Choosing the upper signs and setting $R_{ij} = 0$ these equations coincide with Ref. [11, p. 69].

2.3. Stability conditions

Introducing the complex abbreviations

$$\hat{w}_1 = \hat{u}_1 + \mathrm{j}\hat{v}_1, \quad \hat{w}_2 = \hat{u}_2 \pm \mathrm{j}\hat{v}_2, \tag{16}$$

where $\mathrm{j} = \sqrt{-1}$ is the complex unit, Eq. (15) is equivalent to

$$\dot{\hat{\mathbf{w}}} = \frac{\varepsilon}{\eta_0^2}\begin{bmatrix} -\frac{\eta_0}{2}\Theta_{11} + \mathrm{j}\Omega_1\sigma & \mp\frac{\eta_0}{4\Omega_1}(\Omega_2 R_{12} \pm \mathrm{j}Q_{12}) \\ \mp\frac{\eta_0}{4\Omega_2}(\Omega_1 R_{21} + \mathrm{j}Q_{21}) & -\frac{\eta_0}{2}\Theta_{22} \pm \mathrm{j}\Omega_2\sigma \end{bmatrix}\hat{\mathbf{w}} \tag{17}$$

with the complex state vector $\hat{\mathbf{w}} = [\hat{w}_1, \hat{w}_2]^{\mathrm{T}}$. After rescaling time by ε/η_0^2 the characteristic equation of the coefficient matrix is a complex polynomial of order two

$$\begin{aligned}\lambda^2 + (\tfrac{1}{2}\eta_0(\Theta_{11}+\Theta_{22}) - \mathrm{j}(\Omega_1 \pm \Omega_2)\sigma)\lambda + (\tfrac{1}{2}\eta_0\Theta_{11} - \mathrm{j}\Omega_1\sigma)(\tfrac{1}{2}\eta_0\Theta_{22} \mp \mathrm{j}\Omega_2\sigma) \\ - \frac{\eta_0^2}{16\Omega_1\Omega_2}(\Omega_2 R_{12} \pm \mathrm{j}Q_{12})(\Omega_1 R_{21} + \mathrm{j}Q_{21}) = 0.\end{aligned} \tag{18}$$

Applying the extended Routh–Hurwitz criterion for complex polynomials in Ref. [29], a simplification of the original criterion in Ref. [30], the stability of this polynomial can be determined.

First analysing the case for $\sigma = 0$ in Eq. (10), $\eta = \eta_0$, this polynomial is stable if and only if

$$\Theta_{11} + \Theta_{22} > 0, \tag{19}$$

$$\Theta_{11}\Theta_{22} \pm \frac{Q_{12}Q_{21}}{4\Omega_1\Omega_2} - \frac{R_{12}R_{21}}{4} > \frac{\beta}{(\Theta_{11}+\Theta_{22})^2} > 0, \tag{20}$$

are fulfilled, where

$$\beta = \mp\frac{Q_{12}R_{21}}{4\Omega_2} - \frac{R_{12}Q_{21}}{4\Omega_1}. \tag{21}$$

Note that the interaction term β vanishes in case of a pure stiffness excitation, $R_{ij} = 0$, as well as in case of a pure damping excitation, $Q_{ij} = 0$.

For the general case of $\sigma \neq 0$ in Eq. (10), the following two conditions have to be satisfied for the system being stable:

$$\Theta_{11} + \Theta_{22} > 0, \tag{22}$$

$$a_0\sigma^2 + a_1\{Q_{ij}, R_{ij}\}\sigma + a_2\{Q_{ij}, R_{ij}\} > 0. \tag{23}$$

Note that the conditions in Eqs. (22) and (19) coincide and are independent of the parametric excitation. This condition can be interpret as the main stability condition for damping by parametric excitation. The condition in Eq. (23) defines the critical values

$$\sigma_1 = \widetilde{\sigma}_s - \widehat{\sigma}_{kc} \quad \text{and} \quad \sigma_2 = \widetilde{\sigma}_s + \widehat{\sigma}_{kc} \tag{24}$$

of the detuning σ in Eq. (10) where the frequency shift $\widetilde{\sigma}_s$ and the frequency width $\widehat{\sigma}_{kc}$ are

$$\widetilde{\sigma}_s = \frac{(\Theta_{11}-\Theta_{22})}{2\Theta_{11}\Theta_{22}}\frac{\beta}{2}, \quad \widehat{\sigma}_{kc} = \frac{(\Theta_{11}+\Theta_{22})}{2\Theta_{11}\Theta_{22}}\sqrt{d_{kc}}, \tag{25}$$

and the parametric excitation term d_{kc} is

$$d_{kc} = -\Theta_{11}\Theta_{22}\left(\Theta_{11}\Theta_{22} \pm \frac{Q_{12}Q_{21}}{4\Omega_1\Omega_2} - \frac{R_{12}R_{21}}{4}\right) + \left(\frac{\beta}{2}\right)^2. \tag{26}$$

These critical values determines the stability border in the system parameter space. To decide which side of the boundary is stable and which is unstable the additional condition in Eq. (20) is needed. If this condition is fulfilled then a parametric *anti*-resonance near η_0 with a width of $\widehat{\sigma}_{kc}$ in Eq. (25) is obtained. Otherwise there is

no damping by parametric excitation possible and the vibration amplitudes grow without restriction. These results hold for a first-order perturbation and are valid on the time scale $1/\varepsilon$.

3. General discussion

The stability conditions in the previous section represent the stability of the slow vibrations in the system which enable pertinent interpretations. These conditions were derived for a system with two degrees of freedom only. However, for a perturbation analysis of first order and a parametric excitation at a single frequency η as considered in this contribution, the results can be extended straightforwardly to systems with multiple degrees of freedom.

As shown in Eq. (15), for a system with two degrees of freedom a parametric excitation at $\eta_0 = |\Omega_1 \mp \Omega_2|$ couples the corresponding states u_1, v_1 with u_2, v_2. In analogy to Ref. [31], for a system with n degrees of freedom the same coupling remains and, consequently, in addition to Eq. (15), the uncoupled equations of motion

$$w_i = u_i + \mathrm{j}v_i, \quad \dot{\hat{w}}_i = \frac{\varepsilon}{\eta_0^2}\left\{-\frac{\eta_0}{2}\Theta_{ii} + \mathrm{j}\Omega_i\sigma\right\}\hat{w}_i \quad \text{for} \quad i = 3,\ldots,n, \tag{27}$$

emerge for each degree of freedom that is not affected by parametric excitation, i.e. $i \neq 1, 2$. The necessary and sufficient stability conditions for Eq. (27) are the trivial conditions

$$\Theta_{ii} > 0 \quad \text{for} \quad i \geqslant 3. \tag{28}$$

These conditions can be simply added to the results obtained in the previous section which leads to the stability conditions of a system with multiple degrees of freedom.

3.1. General case

Examining the case where the parametric excitation is not present in the system, $Q_{ij} = 0 = R_{ij}$, the stability conditions in Eqs. (19) and (20) collapse and yield together with Eq. (28)

$$\Theta_{ii} > 0 \quad \text{for} \quad i = 1,\ldots,n. \tag{29}$$

The interaction term β in Eq. (21) vanishes and the parametric excitation term d_{kc} in Eq. (26) becomes negative and leads to purely imaginary critical values of σ in Eq. (24). Hence, the self-excited system without parametric excitation is stable if all modal damping coefficients in the main diagonal of the modal damping matrix are positive or equivalently, the self-excitation is weak and does not destabilise the system. The following cases can be distinguished:

(i) If these conditions hold there is no negative modal damping present in the system and, hence, the system is stable. In this case parametric excitation near a parametric combination frequency η_0 in Eq. (2) may be used to enhance the system damping and vibration suppression is achieved, see the discussion in Ref. [31].
(ii) If one condition in Eq. (29) is violated for $i = 1$ or $i = 2$, $\Theta_{11}\Theta_{22} < 0$, but the less restrictive condition in Eq. (22) is satisfied, the system is unstable but may be stabilised by a proper parametric excitation near the frequency η_0 depending on the condition in Eq. (23).
(iii) In all cases where at least one of these diagonal damping terms vanishes, the system without parametric excitation is on its stability limit, the vibrations are neither damped nor excited but can be stabilised by a proper parametric excitation, according to point (ii).
(iv) Finally, if the conditions in Eq. (29) are violated for $i = 1$ and 2, respectively, the system is unstable and cannot be stabilised by any parametric excitation.

The focus of this study are the cases (ii) and (iii) for which a destabilising self-excitation, $\Theta_{11}\Theta_{22} < 0$, may be stabilised by a proper parametric excitation.

3.2. Single parametric excitation

The extended conditions for vibration suppression in Eqs. (22)–(26) can be simplified to the case of parametric excitation of just one physical parameter as investigated in the literature. For the case of a pure *stiffness* excitation, $R_{ij}=0$, the interaction term β in Eq. (21) vanishes and the parametric excitation term in Eq. (26) becomes

$$d_k=-\Theta_{11}\Theta_{22}\left(\Theta_{11}\Theta_{22}\pm\frac{Q_{12}Q_{21}}{4\Omega_1\Omega_2}\right). \tag{30}$$

Consequently, the frequency shift in Eq. (25) disappears and the critical values of the detuning σ corresponding to Eq. (24) are

$$\sigma_1=-\widehat{\sigma}_k,\quad \sigma_2=\widehat{\sigma}_k. \tag{31}$$

The extended stability conditions in Eqs. (22)–(24) simplify to the equivalent conditions

$$\Theta_{11}+\Theta_{22}>0, \tag{32}$$

$$\widehat{\sigma}_k=\frac{\Theta_{11}+\Theta_{22}}{2}\sqrt{-\frac{\Theta_{11}\Theta_{22}\pm(Q_{12}Q_{21}/4\Omega_1\Omega_2)}{\Theta_{11}\Theta_{22}}}, \tag{33}$$

as derived in Refs. [9–12,14], and summarised in Ref. [31]. It should be mentioned that the critical expression $\widehat{\sigma}_k$ in Eq. (33) was found in Refs. [2,4,5] or [6]. However, since these studies assumed positive damping the main condition in Eq. (32) was not derived and a parametric anti-resonance could not be discovered. As shown in Ref. [31], the conditions in Eqs. (32)–(33) are valid for a system with multiple degrees of freedom if additionally the conditions in Eq. (28) are satisfied.

Similarly, in the case of a pure *damping* excitation, $Q_{ij}=0$, the stability conditions in Eqs. (22)–(24) simplifies into the equivalent conditions

$$\Theta_{11}+\Theta_{22}>0, \tag{34}$$

$$\widehat{\sigma}_c=\frac{\Theta_{11}+\Theta_{22}}{2}\sqrt{-\frac{\Theta_{11}\Theta_{22}-(R_{12}R_{21}/4)}{\Theta_{11}\Theta_{22}}}, \tag{35}$$

as derived in Refs. [20,12]. Although in case of a pure stiffness excitation the stability condition in Eq. (33) is affected by the kind of parametric combination frequency chosen in Eq. (2) this is not the case for a pure damping excitation in Eq. (35). In analogy to Ref. [31] for a pure stiffness variation, these conditions are valid for a system with multiple degrees of freedom if additionally the conditions in Eq. (28) are satisfied.

Note the following facts:

(i) The critical value $\widehat{\sigma}_c$ of a pure damping variation in Eq. (35) is equal at both frequencies $\eta_0=|\Omega_1\mp\Omega_2|$. Consequently, for a given system damping, Θ_{ii} is fixed and $\widehat{\sigma}_c$ depends entirely on the sign of the term $R_{12}R_{21}$ that reflects the symmetry of the parametric excitation matrix $\mathbf{R}$. For a system with a destabilising self-excitation, $\Theta_{11}\Theta_{22}<0$, only a skew-symmetric excitation matrix $\mathbf{R}$ may enhance the radical in Eq. (35) leading to a vibration suppression by parametric excitation near $\eta_0=|\Omega_1\mp\Omega_2|$.

(ii) Contrary to a pure damping variation, the critical value $\widehat{\sigma}_k$ of a pure stiffness variation in Eq. (33) depends on whether the parametric excitation frequency is near $\eta_0=|\Omega_1-\Omega_2|$ or $\eta_0=\Omega_1+\Omega_2$. Now, for a system with a destabilising self-excitation, $\Theta_{11}\Theta_{22}<0$, a parametric anti-resonance may appear near $\eta_0=\Omega_1+\Omega_2$ for a skew-symmetric parametric excitation matrix $\mathbf{Q}$, $Q_{12}Q_{21}<0$, and near $\eta_0=|\Omega_1-\Omega_2|$ for a symmetric excitation matrix $\mathbf{Q}$.

(iii) The stability condition in Eq. (22) of a synchronous stiffness and damping excitation coincides with the stability condition in Eq. (32) or Eq. (34) obtained for a pure stiffness and damping excitation, respectively. Consequently, the main stability condition is preserved.

(iv) In case of a pure stiffness variation, see Eqs. (32) and (33) as well as in case of a pure damping variation, see Eqs. (34) and (35), no additional frequency shift $\widetilde{\sigma}_s$ as in Eq. (24) occurs.

(v) The resultant frequency width $\widehat{\sigma}_{kc}$ in Eq. (25) of the synchronous stiffness and damping excitation is not equivalent to the sum of the frequency widths due to a pure stiffness excitation $\widehat{\sigma}_k$ in Eq. (33) and the frequency width due to a pure damping excitation $\widehat{\sigma}_c$ in Eq. (35),

$$\widehat{\sigma}_{kc} \neq \widehat{\sigma}_k + \widehat{\sigma}_c. \tag{36}$$

3.3. Synchronous parametric excitation

If one demands a design with stability at $\eta_0 = |\Omega_1 - \Omega_2|$ and *simultaneously* at $\eta_0 = \Omega_1 + \Omega_2$ the stability conditions in Eqs. (19)–(20) have to be satisfied for the upper and lower signs, respectively. This requirement demands the following conditions to be satisfied:

$$\Theta_{11} + \Theta_{22} > 0 \quad \text{and} \quad 0 > \Theta_{11}\Theta_{22} > \frac{R_{12}R_{21}}{4} + \frac{(Q_{12}R_{21}/\Omega_2)^2 + (R_{12}Q_{21}/\Omega_1)^2}{16(\Theta_{11} + \Theta_{22})^2}. \tag{37}$$

This means that in the case of a destabilising self-excitation, $\Theta_{11}\Theta_{22} < 0$, it may be possible to stabilise a system at the parametric excitation frequency of the difference type $\eta_0 = |\Omega_1 - \Omega_2|$ and the summation type $\eta_0 = \Omega_1 + \Omega_2$ simultaneously, if at least the necessary condition

$$0 > \Theta_{11}\Theta_{22} > \frac{R_{12}R_{21}}{4} \tag{38}$$

is fulfilled. This requires the parametric damping matrix $\mathbf{R}$ in Eq. (5) to be skew-symmetric and consequently $\mathbf{C}_t$ in Eq. (4). Note that for a pure stiffness excitation simultaneous vibration suppression is not possible, as outlined in Ref. [15]. This result can be concluded straightforwardly in Eq. (38) for $R_{12}R_{21} = 0$.

For a specific system parameter p the stability boundary in the system parameter space projected to the p–η-plane is determined by

$$\eta_0 + \varepsilon\widetilde{\sigma}_s - \varepsilon\widehat{\sigma}_{kc} \leqslant \eta \leqslant \eta_0 + \varepsilon\widetilde{\sigma}_s + \varepsilon\widehat{\sigma}_{kc} \tag{39}$$

following from Eqs. (10) and (24). A graphical interpretation is shown in Fig. 1 that points out the difference between a stiffness excitation, $R_{ij} = 0$, and a synchronous stiffness and damping excitation. The dotted line indicates the stability boundary curve without an additional frequency shift $\varepsilon\widetilde{\sigma}_s$ from the combination resonance frequency η_0 as it would arise for a pure stiffness excitation according to Eq. (33). The solid line indicates the final stability boundary curve resulting for a synchronous excitation according to Eqs. (39) and (25). Consequently, the skeleton line η_0 of the stability boundary curve in case of a pure stiffness excitation is moved to the skeleton line $\eta_0 + \varepsilon\widetilde{\sigma}_s$ in case of a combined synchronous stiffness and damping excitation.

The frequency shift $\widetilde{\sigma}_s$ in Eq. (25) depends on whether the frequency of the stiffness variation is near to a parametric combination frequency of the difference type $\eta_0 = |\Omega_1 - \Omega_2|$ or of the summation type $\eta_0 = \Omega_1 + \Omega_2$. This circumstance results from the expression β in Eq. (21) because the sign of the second

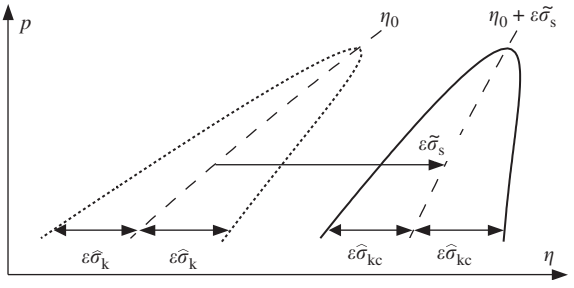

Fig. 1. Shift of stability border in dependence on a system parameter p.

expression in β, $R_{12}R_{21}$, is conserved while the sign of the first expression, $Q_{12}Q_{21}$, alters. Consequently, for a fixed system parameter p the resulting value of the frequency shift $\widetilde{\sigma}_s$ is not the same at the frequencies $\eta_0 = |\Omega_1 \mp \Omega_2|$. Furthermore, if the condition

$$\Omega_1 Q_{12} R_{21} < \Omega_2 R_{12} Q_{21} \tag{40}$$

is fulfilled the resulting sign of $\widetilde{\sigma}_s$ differs, too. This consequence is sketched in Fig. 2 for $A = \Omega_1 Q_{12} R_{21}$, $B = \Omega_2 R_{12} Q_{21}$, $A > B$, and a destabilising self-excitation $\Theta_{11}\Theta_{22} < 0$ with $\Theta_{11} > \Theta_{22}$.

Due to the frequency shift $\widehat{\sigma}_s$ of the stability boundaries the stability conditions in Eqs. (19)–(20) are helpful to determine the stability on the frequency line η_0, but in general they are irrelevant for a classification of the stability domain in the parameter space as performed in Ref. [31] for a pure stiffness variation. The adequate critical conditions for non-vanishing interaction term follows from a stability analysis of the original characteristic polynomial in Eq. (18) by mapping $\sigma \mapsto \widetilde{\sigma}_s + \sigma$, where $\widetilde{\sigma}_s$ is the resulting frequency shift derived in Eq. (25) from the stability analysis at $\eta = \eta_0$, see Ref. [15]. Performing this second stability analysis, the shifted frequency line $\eta_0 + \varepsilon\widetilde{\sigma}_s$ is stable if and only if

$$\Theta_{11} + \Theta_{22} > 0, \quad -\frac{d_{kc}}{\Theta_{11}\Theta_{22}} > 0, \tag{41}$$

are fulfilled instead of Eqs. (19)–(20). Thee inequalities in Eq. (41) enable an elegant classification of the conditions in Eqs. (19), (20), and (24) for a synchronous damping and stiffness variation that is summarised in Table 1. These and the following results for a two-degrees-of-freedom system can be extended easily to a system with multiple degrees of freedom if additionally the conditions in Eq. (28) are met.

Table 1 shows the qualitative stability map in dependency of an arbitrary system parameter p and the parametric excitation frequency η for a non-vanishing interaction term β. Read this table by either using always the upper sign or always the lower sign in analogy to the previous calculations. Plotting the frequency $\eta_0 = |\Omega_1 \mp \Omega_2|$ as a function of a system parameter p results in a frequency line. The frequency shift $\widetilde{\sigma}_s$ is drawn for a positive interaction term β and $\Theta_{11} > \Theta_{22}$. If the conditions in Eq. (41) are violated then the system becomes unstable for parameter values p lying on the shifted frequency line $\eta_0 + \varepsilon\widetilde{\sigma}_s$. This is shown in the left column in Table 1. If additionally the stability conditions in the general case from Eq. (29) are violated, then the system is unstable on the shifted frequency line as well as in the remaining parameter domain and the stability width $\widehat{\sigma}_{kc}$ is purely imaginary, see left bottom cell. On the other hand, if the conditions in Eq. (29) are satisfied, the system is unstable in the vicinity of the shifted frequency line $\eta_0 + \widetilde{\sigma}_s$ and stable in the remaining parameter domain, see left top cell. In this case the frequency η_0 is called a parametric resonance frequency,because it disturbs an otherwise stable system.

For a stable frequency line $\eta_0 + \varepsilon\widetilde{\sigma}_s$ the conditions in Eqs. (19) and (20) are satisfied for the upper or the lower signs. This is shown in the right column in Table 1. Now if the general stability conditions in Eq. (29) are satisfied then the system is stable in the whole parameter domain, see right top cell. On the other hand, if the general stability conditions are violated, the system remains stable in the vicinity of the frequency line but

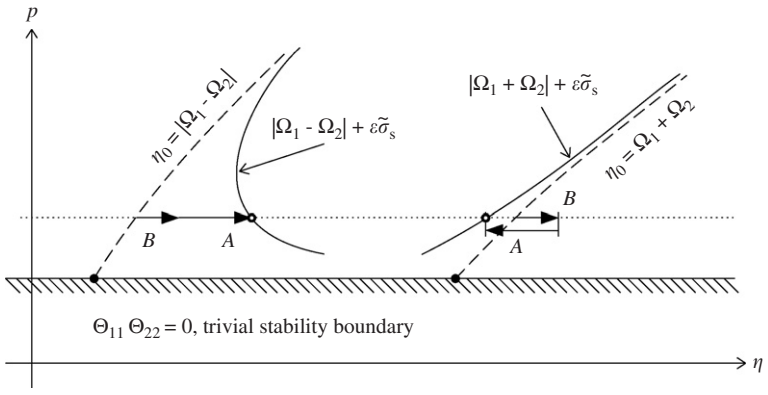

Fig. 2. Shift of skeleton lines if the condition in Eq. (40) is satisfied and $\Theta_{11} > \Theta_{22}$, $\Theta_{11}\Theta_{22} < 0$.

Table 1
Summary for synchronous stiffness and damping excitation at parametric combination resonance frequencies with sketches for a positive interaction term β and $\Theta_{11} > \Theta_{22}$

	unstable $\eta_0 + \varepsilon\widetilde{\sigma}_s$	stable $\eta_0 + \varepsilon\widetilde{\sigma}_s$
	$\Theta_{11} + \Theta_{22} > 0, \quad -\dfrac{d_{kc}}{\Theta_{11}\Theta_{22}} < 0$	$\Theta_{11} + \Theta_{22} > 0, \quad -\dfrac{d_{kc}}{\Theta_{11}\Theta_{22}} > 0$
$\Theta_{11}\Theta_{22} > 0$	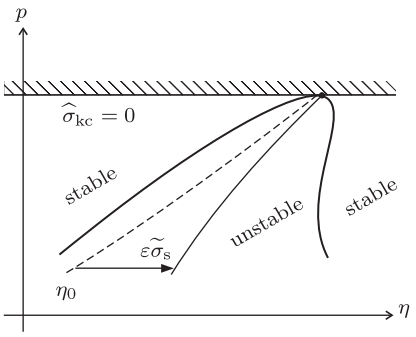 real-valued $\widehat{\sigma}_{kc}$ **parametric resonance**	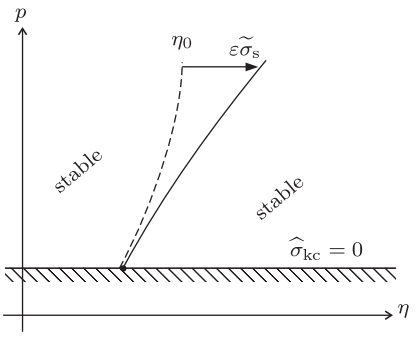 purely imaginary $\widehat{\sigma}_{kc}$ **stable**
$\Theta_{11}\Theta_{22} < 0$	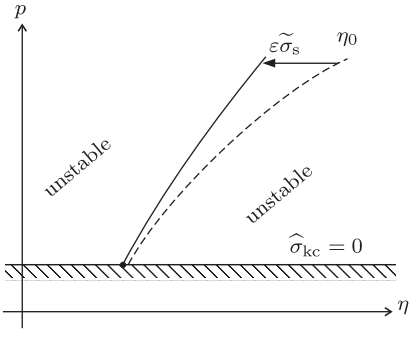 purely imaginary $\widehat{\sigma}_{kc}$ **unstable**	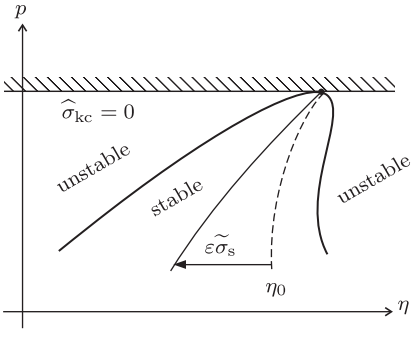 real-valued $\widehat{\sigma}_{kc}$ **parametric anti-resonance**

becomes unstable in the remaining parameter domain, see right bottom cell. In this case the frequency η_0 is called a parametric *anti*-resonance frequency, because it stabilises an otherwise unstable system.

Comparing the two left cells reveals that passing the critical condition $\Theta_{11}\Theta_{22} = 0$ from $\Theta_{11}\Theta_{22} > 0$ to $\Theta_{11}\Theta_{22} < 0$ by varying a system parameter p leads to a change of the sign of the frequency shift $\widetilde{\sigma}_s$. Additionally, a positive parametric excitation term d_{kc}, corresponding to a real-valued stability width $\widehat{\sigma}_{kc}$, switches to a negative parametric excitation term, corresponding to a purely imaginary stability width. Generally, if a system parameter p fulfills this switching condition $\Theta_{11}\Theta_{22} = 0$, then the stability on the shifted frequency line $\eta_0 + \varepsilon\widetilde{\sigma}_s$ switches from stable to unstable or vice versa. This fact is indicated by a hatched border. Reaching this border for such a critical parameter value, the corresponding column have to switched.

The case where $\Theta_{11}+\Theta_{22}<0$ is valid leads always to an unstable system. In this case the stability map for a certain parameter looks like in the sketch in the left bottom corner in Table 1.

4. Example system

A two-mass system with spring- and damper-elements as drawn in Fig. 3 is considered, which is an extension of the originally investigated systems in Refs. [21,32]. The system possesses two degrees of freedom: the vertical positions z_1, z_2 of the two masses. The top mass m_2 is connected by a linear spring k_2 to the bottom mass m_1. A constant flow U generates a self-exciting force which acts on mass m_2 in direction z_2. The subsystem m_2, k_2 rests on a base mass m_1 which is attached to the inertial reference frame by a spring-element $k_1(\tau)$ and a viscous damping element $c_1(\tau)$. This system may represent a model of the first two modes of a mechanical structure with corresponding modal masses. The stiffness and damping coefficient of the suspension consist of a constant and a controlled small time-dependent component

$$k_1(\tau)=k_0(1+\varepsilon_k\cos(\eta\tau)) \quad \text{and} \quad c_1(\tau)=c_0(1+\varepsilon_c\cos(\eta\tau)). \tag{42}$$

Since there is no phase difference, both coefficients are varied synchronously in time. The flow-induced self-excitation force due to the constant flow velocity U is modelled by a linear negative damping coefficient resulting from a linearised van der Pol or Rayleigh model

$$F_{se}=(c_{se}-d_{se}U^2)\dot{z}_2. \tag{43}$$

For the two mass system that is under the simultaneous influence of self-excitation and parametric excitation as shown in Fig. 3 the equations of motion are given by

$$\begin{bmatrix} m_1 & 0 \\ 0 & m_2 \end{bmatrix}\ddot{\mathbf{z}}+\begin{bmatrix} c_1(\tau) & 0 \\ 0 & c_{se}-d_{se}U^2 \end{bmatrix}\dot{\mathbf{z}}+\begin{bmatrix} k_1(\tau)+k_2 & -k_2 \\ -k_2 & k_2 \end{bmatrix}\mathbf{z}=\begin{bmatrix} 0 \\ 0 \end{bmatrix} \tag{44}$$

with the state vector $\mathbf{z}=[z_1(\tau),z_2(\tau)]^{\mathrm{T}}$. For this simple system the parametric excitation matrix is symmetric, in which case vibration suppression may be achieved for a pure stiffness excitation near $\eta_0=|\Omega_1-\Omega_2|$ only, see Section 2.3 and Ref. [15] for more details. However, a pure damping variation with a symmetric parametric excitation matrix always destabilises the system. The question arises whether the parametric *anti*-resonance due to the stabilising stiffness excitation or the resonance due to the destabilising damping excitation will dominate.

In order to examine the analytical results obtained for vibration suppression, the dynamic behaviour of the system in Eq. (44) is compared for different kinds of parametric excitations: a pure harmonic stiffness variation and the investigated synchronous stiffness and damping variation. Since the stability analysis in the previous section was performed for the normal form in Eq. (5) the equation of motion in Eq. (44) has to be transformed according to Eqs. (7) and (9). The following non-dimensional parameters are introduced in order to decrease the number of system parameters for the numerical analysis

$$M=\frac{m_2}{m_1}, \quad \kappa_1=\frac{c_0}{m_1\omega_2}, \quad \kappa_2=\frac{c_{se}-d_{se}U^2}{m_1\omega_2}, \quad Q^2=\frac{k_0}{m_1\omega_2^2}, \quad \varepsilon_k, \quad \text{and} \quad \varepsilon_c \tag{45}$$

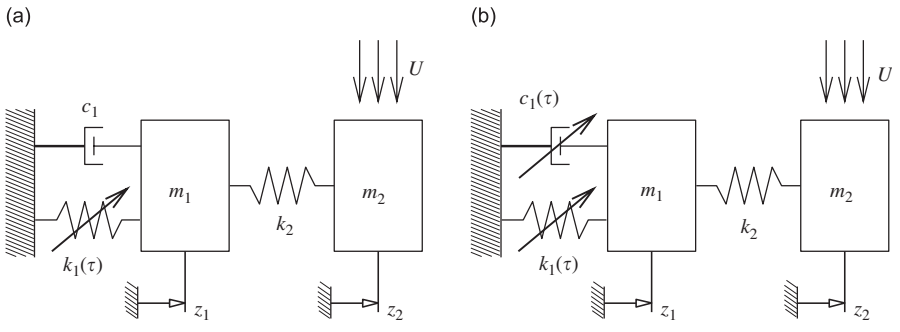

Fig. 3. Two mass system with a pure stiffness variation (a) or a synchronous stiffness and damping variation (b).

with the undamped natural frequency of subsystem 2, $\omega_2 = \sqrt{k_2/m_2}$, and the mass ratio M and frequency ratio Q. These parameters represent relations between the dimensional physical system parameters. For a certain physical system specific values for some of the parameters have to be chosen additionally.

To verify the results of the analytical analysis an exact method based on Floquet's theorem is used in combination with numerical time integration (see Ref. [16] for details). By numerically integrating the system equations in Eq. (44) for fixed system parameters the monodromy matrix after one period of the parametric excitation is calculated. The eigenvalues of the monodromy matrix determine the stability of the system. For systems with a larger number of degrees of freedom, the numerical procedure proposed in Ref. [33] is computationally more efficient.

For the equations of motion in Eq. (44) the sum of the modal damping coefficients in the main stability condition in Eqs. (32), (34) and (41) can be rewritten as

$$\Theta_{11} + \Theta_{22} = \kappa_1 + M\kappa_2 > 0. \tag{46}$$

Resulting from the second inequality in Eq. (26), a non-dimensional excitation ratio r between the stiffness and damping excitation can be defined and expressed by the parameters introduced in Eq. (45)

$$r = \frac{\Omega_1 Q_{12} R_{21} + \Omega_2 R_{12} Q_{21}}{Q_{12} Q_{21} - \Omega_1 \Omega_2 R_{12} R_{21}} = \frac{\varepsilon_k \varepsilon_c \kappa_2 Q(1 + M + Q^2)}{(\varepsilon_c \kappa_2)^2 - \varepsilon_k^2 Q^3}. \tag{47}$$

This ratio is an indicator for the strength of the damping variation R_{ij} with respect to the stiffness excitation Q_{ij}. The effects of the stiffness excitation exceed the effect of the damping excitation if $r \lessapprox 1$ and vice versa if $r \gtrapprox 1$. For $r \lessapprox 1$ the stability gained by pure stiffness variation is conserved while for $r \gtrapprox 1$ the destabilising damping variation outweighs the otherwise stable pure stiffness variation. A good approximation for the excitation ratio in Eq. (47) can be obtained if the interaction term β is neglected and only the left-hand side of the second inequality in Eq. (26) is taken into account

$$\tilde{r} = \frac{\Omega_1 \Omega_2 R_{12} R_{21}}{Q_{12} Q_{21}} = \frac{(\varepsilon_c M \kappa_2)^2}{\varepsilon_k^2 Q^3}. \tag{48}$$

Two numerical sets as listed in Table 2 are investigated that both satisfy the condition in Eq. (46). Initially the numerical set for the weakly damped system A is analysed. Figs. 4 and 5 show stability charts for a pure harmonic stiffness excitation and for a synchronous stiffness and damping excitation, respectively, in dependency of the non-dimensional system parameter Q in Eq. (45) and the frequency ratio η/ω_2, where η is the parametric excitation frequency as defined in Eq. (4). The shadowed area indicates the numerically calculated stability area. The bold solid line shows the analytical stability border calculated from Eqs. (32)–(33) in Fig. 4 and from Eqs. (22)–(23) in Fig. 5. Although from a mathematical point of view the scaling parameters ε_k, ε_c in Eq. (45) are not small as assumed in the analytical stability analysis the stability conditions obtained still accurately reproduce the system behaviour.

For the system without parametric excitation, $\varepsilon_k = 0 = \varepsilon_c$, the trivial stability boundary according to Eq. (29), $\Theta_{11}\Theta_{22} = 0$, leads to the critical stiffness ratio $Q_{\text{crit}} = 1.73$. For a frequency ratio $Q > Q_{\text{crit}} = 1.73$, the modal damping parameter Θ_{22} is negative and system A is dynamically unstable due to self-excitation even without the parametric excitation operating. By activating a parametric excitation, $\varepsilon_k \neq 0$, it is possible to suppress the system vibrations due to a destabilising self-excitation. Such a parametric excitation deforms the trivial stability boundary $Q = Q_{\text{crit}}$ as is shown in Figs. 4 and 5 leading to regions of stability and instability, respectively.

Table 2
Non-dimensional parameters

	M	κ_1	κ_2	ε_k	ε_c
System A	0.5	0.05	−0.01	0.3	0.5
System B	5	0.5	−0.1	0.3	1

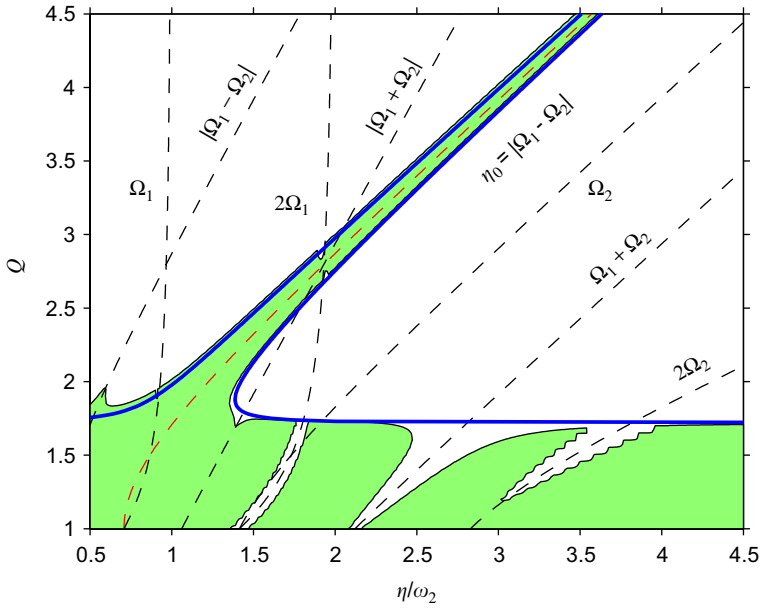

Fig. 4. Comparison of analytical and numerical analysis of Q–η-stability chart for pure harmonic stiffness excitation ($\varepsilon_c = 0$) in system A: shaded region numerical, solid line analytical result.

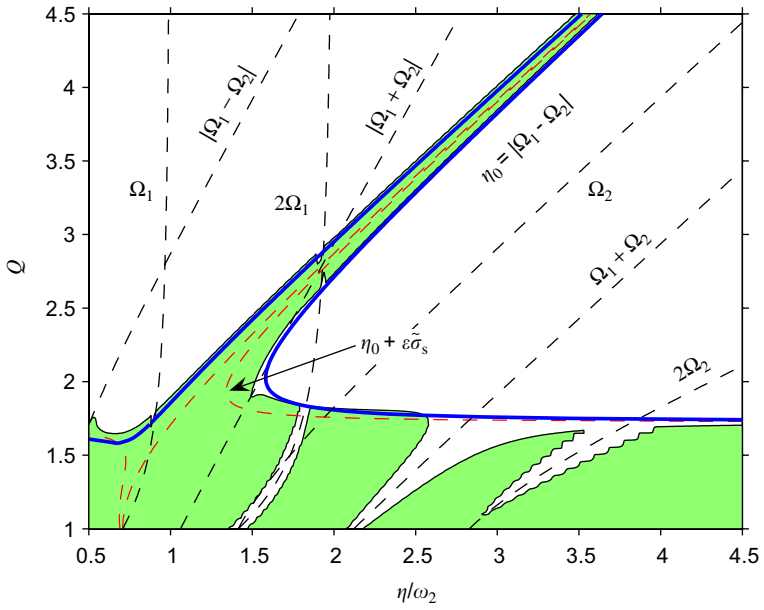

Fig. 5. Comparison of analytical and numerical analysis of Q–η-stability chart for synchronous stiffness and damping excitation in system A: shaded region numerical, solid line analytical result.

A key to the interpretation of the results are the parametric resonance frequencies of the first kind $2\Omega_{1,2}/N$ and those of the second kind $|\Omega_1 \pm \Omega_2|/N$, with $N = 1, 2$ (see Eq. (2)). These frequency curves are plotted as dashed lines. If the excitation frequency η is equal to the parametric *anti*-resonance frequency $\eta_0 = |\Omega_1 - \Omega_2| + \varepsilon\tilde{\sigma}_s$ the vibration can be suppressed successfully. On the other hand, choosing an arbitrary value of η outside the shaded area results in increasing vibrations due to the destabilising self-excitation. An additional but small stability area is caused by the second-order anti-resonance frequency $|\Omega_1 - \Omega_2|/2$. Analytical and

numerical results agree amazingly well in the vicinity of the main anti-resonance frequency. For $Q<Q_{\text{crit}}$ the initially stable system is destabilised near the parametric resonance frequencies and the stability area is destroyed. For $Q>Q_{\text{crit}}$ the system is unstable due to the self-excitation and additionally unstable near the parametric resonance frequencies where the vibration amplitudes grow faster than without any parametric excitation present in the system. However, near the main parametric anti-resonance frequencies $|\Omega_1-\Omega_2|$ the system vibrations are suppressed successfully in regions within the conventional system without periodic control of one or more system parameters is unstable. A stable frequency ratio of 7.8 can be achieved.

Comparing Figs. 4 and 5 reveals the effect of the additional shift as predicted by Eq. (39). Due to the additional synchronous damping variation the original skeleton line η_0 in Fig. 4 is modified by the additional shift $\varepsilon\widetilde{\sigma}_s$ in Fig. 5 as outlined in Fig. 1. Furthermore, although a pure damping variation is always destabilising for the system chosen, in combination with a synchronous stiffness variation even a small improvement near $\eta=1.5$ is obtained. On the other hand, the adaption of the skeleton line leads to a loss of stability near $\eta=0.7$. For the weakly damped system A the stability region gained and created by the stiffness variation, is only disturbed but not destroyed by the interaction with the destabilising damping variation. The stable parametric anti-resonance domain is conserved, in some regions near the trivial stability boundary even enlarged. The analytical analysis predicts an additional shift of the skeleton line of the stability boundary due to the combination of stiffness and damping variation that explains the small loss in and the small enlargement of the stable domain. Note that the results derived in the previous section can be applied to predict instability regions near $\eta_0=\Omega_1+\Omega_2$ and give the same accuracy as the prediction of stability gain near $\eta_0=|\Omega_1-\Omega_2|$. The stability boundaries are not plotted to keep the stability map clear.

For system A the excitation ratio defined in Eq. (48) is very small within the parameter range of $Q, r, \widetilde{r}\ll 1$, which corresponds to a weak interaction of both excitations. In this case a disturbance of the stability gain near $\eta_0=|\Omega_1-\Omega_2|$ can be recognised only close to the trivial stability boundary $\Theta_{11}\Theta_{22}=0$, at which the denominators in Eq. (25) vanish. Choosing the second parameter set in Table 2 representing the strongly damped system B, the excitation ratio in Eq. (48) becomes 1 at $Q_{\tilde{r}}=1.41$. The exact ratio in Eq. (47) yields $Q_r=1.76$. The stabilising effect of the stiffness excitation exceeds the destabilising effect of the damping excitation for $Q>Q_r$ and vice versa for $Q<Q_r$.

Stability maps of the strongly damped system B are shown in Figs. 6 and 7. Now the stability gain by parametric anti-resonance does not cover such a large value range of Q as for the system A in Figs. 4 and 5.

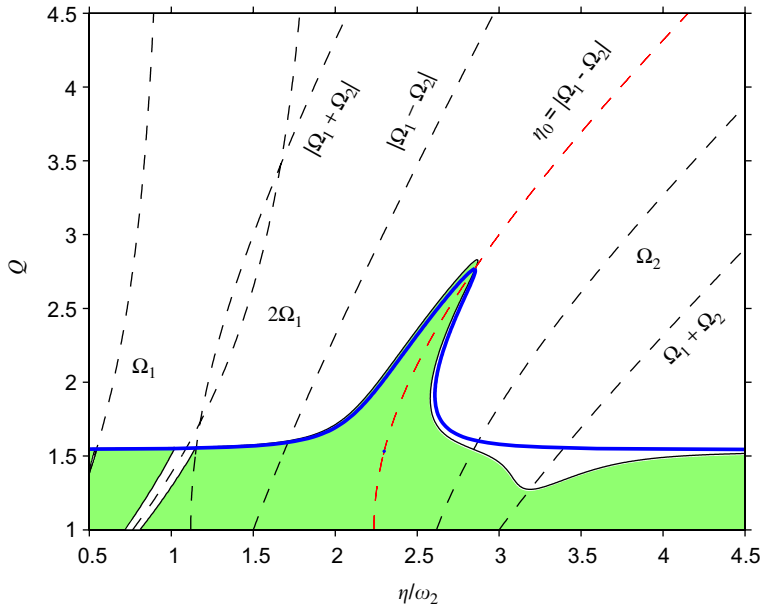

Fig. 6. Comparison of analytical and numerical analysis of Q–η-stability chart for pure harmonic stiffness excitation ($\varepsilon_c=0$) in system B: shaded region numerical, solid line analytical result.

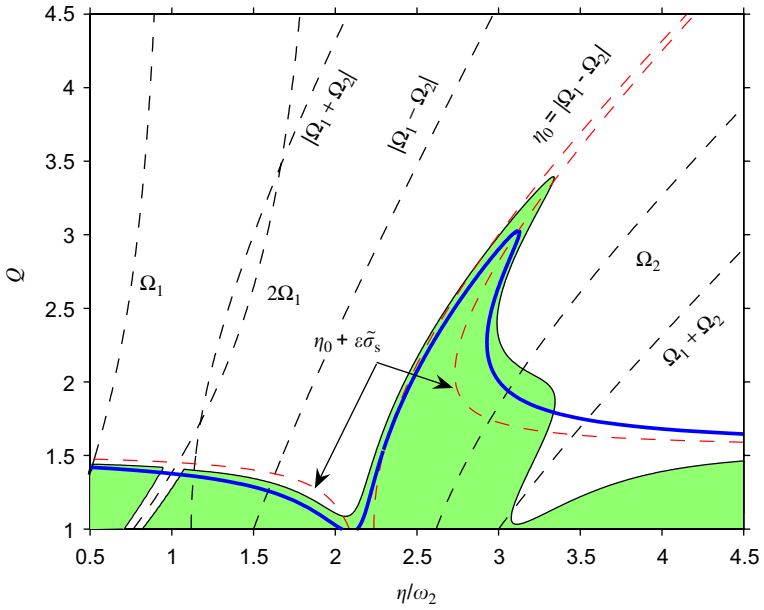

Fig. 7. Comparison of analytical and numerical analysis of Q–η-stability chart for synchronous stiffness and damping excitation in system B: shaded region numerical, solid line analytical result.

For the system without parametric excitation, $Q_{ij} = 0 = R_{ij}$, the trivial stability boundary $\Theta_{11}\Theta_{22} = 0$ leads to the critical stiffness ratio $Q_{\text{crit}} = 1.54$. In case of a pure stiffness variation the analytical predictions agree well with the numerical results although the perturbation analysis was performed under the assumption of small damping, see Fig. 6. In case of the synchronous damping and stiffness variation the assumption of small damping in the analytical stability analysis becomes evident, see Fig. 7. In this case the analytical predictions fail quantitatively but are capable to explain the stability map qualitatively. In fact the stability gained by parametric anti-resonance in Fig. 6 is shifted towards the new skeleton line $\eta_0 + \varepsilon\tilde{\sigma}_s$ in Fig. 7 so much that the stability gain at the anti-resonance frequency $\eta_0 = |\Omega_1 - \Omega_2|$ disappears. The stability boundary is modified strongly, particularly near the trivial stability boundary Q_{crit}, however, the parametric anti-resonance itself is conserved. In more detail the stabilising effect of the stiffness excitation exceeds the destabilising effect of the damping excitation for $Q > Q_r$ and vice versa for $Q < Q_r$. From the numerical point of view it may appear that the parametric anti-resonance at η_0 is destroyed but the analytical investigation shows that the anti-resonance is actually shifted.

Summarising, the analytical predictions outlined in the previous section are confirmed and explain the numerical results in great detail. It was shown that if a self-excited system can be stabilised by a pure stiffness excitation it can be stabilised by a synchronous stiffness and damping excitation, too. The stability gain is conserved. The main difference between these excitations is the location of the anti-resonance frequency that is shifted from regions in the vicinity of the skeleton line η_0 to the skeleton line $\eta_0 + \varepsilon\widehat{\sigma}$. The interaction between stiffness and damping excitation is crucial in the vicinity of the trivial stability boundary $\Theta_{11}\Theta_{22} = 0$ and becomes smaller with increasing distance from this boundary. In common mechanical structures the system damping is much smaller than the stiffness, $c_1 \ll k_1$, in which case the interaction of the parametric excitations is weak, $r, \tilde{r} \ll 1$, and the anti-resonance effect remains close to the skeleton line η_0, similar to Fig. 5. It is worth to mention that if the pure stiffness excitation as well as the pure damping variation are resonant, a parametric anti-resonance cannot be created by interaction of both excitation in a synchronous stiffness and damping excitation.

5. Conclusions

Systems with two and more degrees of freedom under the simultaneous influence of self-excitation and parametric excitation by synchronous stiffness and damping excitation are examined. From previous studies it

is known that a harmonic stiffness excitation with a frequency near the combination resonance frequency of the system can stabilise an otherwise unstable system. In the present study general conditions for vibration suppression are derived analytically for a synchronous stiffness and damping variation. These analytical stability conditions enable a deeper understanding of the interaction of different kinds of parametric excitation. The great benefit of the analytically approximated stability boundary curves is the elegant classification of the stabilising effect of a parametric anti-resonance in the context of a classical parametric resonance.

The analytically approximated predictions are compared to numerical time integration of the original equations of motion for weakly and strongly damped mechanical systems. It is shown that for symmetric excitation matrices a gain of stability domain created by a stiffness excitation may only be disturbed but not destroyed by the interaction with a destabilising damping excitation. The main stable domain is conserved, in some region even enlarged. The analytical analysis shows an additional shift of the skeleton line of the stability boundary due to the interaction of stiffness and damping variation that explains the small loss and the small enlargement of the stable domain.

The results demonstrate that parametric excitation at an appropriate frequency can be employed to extend significantly the area of stability of systems with self-excitation even in case of a synchronous parametric excitation. The proposed control strategy shows great potential being employed in practical applications when a destabilisation due to self-excitation occurs or when the damping of transient vibrations in weakly damped systems shall be enhanced.

Acknowledgement

This contribution is based on research that was supported by the Austrian Science Fund (FWF) within Project P16248.

References

[1] V.V. Bolotin, *Dynamic Stability of Elastic Systems*, Holden-Day, San Francisco, 1964.
[2] T. Yamamoto, A. Saito, On the vibrations of summed and differential types under parametric excitation, *Memoirs of the Faculty of Engineering* 22 (1) (1970) 54–123.
[3] V.A. Yakubovich, V.M. Starzhinskii, *Linear Differential Equations with Periodic Coefficients* (two volumes), Wiley, London, 1975.
[4] N. Eicher, *Einführung in die Berechnung parametererregter Schwingungen*, Technical University of Berlin, TUB-Documentation, 1981 (in German).
[5] M. Cartmell, *Introduction to Linear Parametric and Nonlinear Vibrations*, Chapman & Hall, Englewood Cliffs, NJ, 1990.
[6] A. Seyranian, A. Mailybaev, *Multiparameter Stability Theory with Mechanical Applications, Stability, Vibration and Control of Systems*, Vol. 13, World Scientific, Singapore, 2003.
[7] J. Warminski, J.M. Balthazar, Vibrations of a parametrically and self-excited system with ideal and non-ideal energy sources, *Journal of the Brazilian Society of Mechanical Sciences and Engineering* 25 (4) (2003) 413–420.
[8] A. Tondl, On the Interaction between Self-excited and Parametric Vibrations. National Research Institute for Machine Design, Prague, Monographs and Memoranda, Vol. 25, 1978.
[9] A. Tondl, To the problem of quenching self-excited vibrations, *Acta Technica CSAV* 43 (1998) 109–116.
[10] S. Fatimah, F. Verhulst, Suppressing flow-induced vibrations by parametric excitation, *Nonlinear Dynamics* 23 (2003) 275–297.
[11] Abadi, Nonlinear Dynamics of Self-excitation in Autoparametric Systems, PhD Thesis, Utrecht University, 2003.
[12] F. Dohnal, Application of the averaging method on parametrically excited 2dof-systems, Technical Report, Institute for Machine Dynamics and Measurement, Vienna University of Technology, Austria, 2003.
[13] A. Tondl, *Quenching of Self-excited Vibrations*, Academy of sciences, Czech Republic, 1991.
[14] A. Tondl, H. Ecker, Cancelling of self-excited vibrations by means of parametric excitation, *Proceedings of the ASME Design Engineering Technical Conference* (*DETC*), Las Vegas, Nevada, September 1999.
[15] F. Dohnal, Damping of Mechanical Vibrations by Parametric Excitation, PhD Thesis, Vienna University of Technology, 2005.
[16] K. Makihara, H. Ecker, F. Dohnal, Stability analysis of open-loop stiffness control to suppress self-excited vibrations, *Journal of Vibration and Control* 11 (2005) 643–669.
[17] F. Dohnal, W. Paradeiser, H. Ecker, Experimental Study on Cancelling Self-Excited Vibrations by Parametric Excitation, *Proceedings of ASME International Mechanical Engineering Conferences and Exposition*, IMECE, Chicago, IL, November 2006.
[18] W. Paradeiser, Experimenteller Nachweis einer Parameter-Antiresonanz, Diploma Thesis, Vienna University of Technology, 2006 (in German).
[19] S. Bittanti, P. Colaneri, *Proceedings of the First IFAC Workshop on Periodic Control Systems*, Cernobbio-Como, Italy, 2001.

[20] A. Tondl, Combination resonances and anti-resonances in systems parametrically excited by harmonic variation of linear damping coefficients, *Acta Technica CSAV* 3 (2003) 239–248.
[21] F. Dohnal, Suppression of self-excited vibrations by synchronous stiffness and damping variation, *Proceedings of the Dynamics of Machines*, Prague, February 2005, pp. 23–30.
[22] R. Mickens, *An Introduction to Nonlinear Oscillations*, Cambridge Press, Cambridge, 1981.
[23] A.H. Nayfeh, D.T. Mook, *Nonlinear Oscillations*, third ed., Wiley, New York, 1995.
[24] J.J. Thomsen, *Vibrations and Stability—Advanced Theory Analysis and Tools*, second ed., Springer, Berlin, Heidelberg, New York, 2003.
[25] I.I. Blekhman, *Selected Topics in Vibrational Mechanics, Stability, Vibration and Control of Systems*, Vol. 11, second ed., World Scientific, Singapore, 2004.
[26] S.C. Sinha, E. Butcher, Symbolic computation of fundamental solution matrices for linear time-periodic systems, *Journal of Sound and Vibration* 206 (1997) 61–85.
[27] J.J. Thomsen, Some general effects of strong high-frequency excitation: stiffening, biasing and smoothening, *Journal of Sound and Vibration* 253 (4) (2002) 807–831.
[28] F. Verhulst, *Nonlinear Differential Equations and Dynamical Systems*, *Texts in Applied Mathematics*, Vol. 50, Springer, Berlin, Heidelberg, New York, 2000.
[29] F. Gantmacher, *Matrizenrechnung Teil II, Spezielle Fragen und Anwendungen*, Hochschulbücher für Mathematik, VEB Deutscher Verlag der Wissenschaften, Berlin, 1966 (in German).
[30] H. Bilharz, Bemerkung zu einem Satze von Hurwitz, *Zeitschrift für Angewandte Mathematik und Mechanik (ZAMM), Applied Mathematics and Mechanics* 24 (2) (1944) 77–82 (in German).
[31] F. Dohnal, Damping by parametric stiffness excitation—resonance and anti-resonance, *Journal of Vibration and Control* 2007, accepted for publication.
[32] F. Dohnal, H. Ecker, A. Tondl, Vibration control of self-excited oscillations by parametric stiffness excitation, *Proceedings of the 11th International Congress of Sound and Vibration* (*ICSV11*), St. Petersburg, July 2004, pp. 339–346.
[33] W.T. Wu, J.H. Griffin, J.A. Wickert, Perturbation method for the Floquet eigenvalues and stability boundary of periodic linear systems, *Journal of Sound and Vibration* 182 (2) (1995) 245–257.